Engineering Journal of the University of Qatar, Vol. 13, 2000, pp.

A NEW THREE NODES SHELL ELEMENT WITH TRANSVERSE SHEAR

Guenfoud Mohamed
Institut De Génie-Civil
Université De Guelma
BP 401, Guelma 24 000
Algerie

ABSTRACT

This paper proposes a new three node curved shell element. The approach used in the development of the new element is based on the Marguerre shallow shell theory which incorporates the effects of initial curvature (out-of plane displacement) of the shell but avoids locking and kinematic mode created by the coupling between the membrane and the bending deformations. The decomposition mode technique is used to alleviate the membrane locking problem and also to improve the membrane bending performance. In the formulation of the new element, the Mindlin-Reissner kinematic hypothesis is adopted to include the transverse shear effect. The Discrete Strain Theory (DST) is used to avoid the shear locking problem found in thin shells. The resulting element is the superimposition of the Constant Strain Triangle (CST) element on the Discrete Shear Triangle (DST) element. This formulation enables us to obtain a shell element, which does not produce spurious singular modes, avoids locking phenomena, and excels in calculation efficiency. The results of several examples show that, the proposed shell elements accuracy and convergence of the proposed numerical modelieure quite satisfactory, desipite its simplicity.

KEY WORDS : Shear locking, membrane locking, decomposition mode technique, Marguerre's theory, discrete strain.

INTRODUCTION

The construction of a simple and efficient numerical model for curved structures modelling is an important subject,which is still of interest to researchers . Generally, two problems are encountered during the modeling of curved structures. The first one is the geometrical representation of the structure,which is solved by the Marguerre shallow shell theory (incorporates the effects of the initial deflection in the strain tensor). The coupling between membrane end bending deformations creates the membrane locking phenomenon which is treated by the decomposition mode technique [1], [2] and [3]. The second one is the identification of the transverse shear and membrane locking phenomenon effects [2] and [4]. The type of shear locking is associated with the overconstraining effect of the condition of zero transverse shear strain energy on the assumed displacement field for thin shells. The membrane locking is due to the overconstraining effect of the condition of zero membrane strains for curved shells. These problems are more critical for lower-order elements, which are preferred in the analysis of nonlinear problems because of their simplicity and modleing easiness .

To alleviate these deficiencies, several methods have been proposed by many investigators in the past such as the Selective and Reduced Integration schemes [5], [6], Heterosis elements [6], Stabilization methods [3], and Discrete Kirchhoff elements [7], etc.

With the aformentioned developments, it is possible to obtain a number of successful C° displacement-based shell elements. These approaches, however, provide a number of limitations. The selective or reduced integration scheme is not always successful in overcoming the locking problem . Thus, the resulting solutions may be overstiff for problems with highly constrained boundaries when coarse meshes are used. Furthermore, these schemes may engender rank deficiency for problems with lightly constrained boundries [3], [5]. Heterosis elements exhibit overstiffening effects for problems with irregular mesh [8]. The stabilization methods involve certain parameters which still lack appropriate physical interpretations. Discrete Kirchhoff elements (DKT, DKQ) do not include transverse shear deformation effects. These elements restrict transverse shear deformations (situations always enwantered in the sandwich and laminated composite structures).

Lardeur and Batoz [7] developed the Discrete Shear Triangle (DST) plate element element which is, highly satisfactory in flexure. The formulation of the DST plate element is based on a generalization of the Discrete Kirchhoff Technique to include transverse shear effects. It coincide with the DKT (Discrete Kirchhoff Triangular) plate element if the shell thickness becomes thin. The purpose of the present paper is to combine both the (DST) plate element and the Constant Strain Triangular (CST) membrane element and taking into account an initial curvature (according to the Marguerre's theory). The resulting shell element is called Discrete Shear Triangle in Marguerre theory (DSTM). This element is applicable to both thin and thick shells and can be easily implemented and incorporated into existing finite element analysis programs with minimum modification. In this paper, we first present the Marguerre shallow shell theory and its advantages in solving curved structures. The linear generation of the mesh will then be presented (i.e., the definition of the reference axes, information on area coordinates and description of the membrane and flexural behavior). Special attention was paid to the coupling between membrane and flexural behaviour, in order to avoid membrane locking and the coupling between flexural and shearing behaviour in order to alleviate the shear locking. Numerical examples are presented to evaluate the performance of the developed element .The proposed element,which has no hourglass modes, has a rapid convergence, provides a reasonable stress accuracy , and also improves the membrane bending behaviour of the shell.

MARGUERRE SHALLOW SHELL THEORY

Introduction

The two main approaches used for solving the linear analysis of curved structures are :

1. The facet approximation approach by flat elements, which presents a simple formulation but requires generally a high computer cost. This is caused by the fine discretization necessary for correctly modelling the curved geometry.

2. The shell element approach whose first advantage is the correct modelisation of the curved geometry. However, its manipulation is often difficult especially when using curvilinear coordinates.

The Marguerre's theory is in partial agreement with above- mentioned these points. Indeed, this theory is used for shallow shell elements and allows convergence towards deep shell solution [9]. This is not the case for an element developed in curvilinear coordinates with a shallow shell theory [9]. The computation is performed in Cartesian coordinate and on a straight configuration.

The Marguerre's theory and its exceptional ability in obtaining accurate numerical solution to general shell problems is introduced here in. for more details the reactor is referred to [1],[2],and [3].

General Idea of Marguerre's Theory

This theory was developed for shallow shells. It considers that the undeformed shell configuration is obtained after a fictitious displacement of the plate. The effects of this fictitious displacement are introduced as an initial deflection w_0 in the linear part of the strain tensor. The computation is performed on a Co-rotational system of axes, which gives a correct representation of rigid body motion.
The modified strain tensor for a plate can be expressed as :

$$\varepsilon_{ij} = \frac{1}{2}\left(\frac{\partial u_i}{\partial x_j} + \frac{\partial u_j}{\partial x_i}\right) - z\left(\frac{\partial^2 w}{\partial x_i \partial x_j}\right) + \left(\frac{\partial w_0}{\partial x_i}\right)\left(\frac{\partial w}{\partial x_j}\right) \tag{1}$$

with :
$$\frac{\partial^2 w_0}{\partial x_i^2} \ll 1 \qquad \frac{\partial^2 w_0}{\partial x_j^2} \ll 1 \tag{2}$$

The terms with $\frac{\partial w_0}{\partial x_i}$ are the membrane terms induced by the initial curvature w_0.
This curvature creates the coupling between membrane and bending. In this case the inextensional bending mode cannot be represented exactly. This phenomenon is called the membrane locking. The use of the decomposition mode technique prescribed by Stolarski et al [10] solves this problem. It consists of correctly defining the relation ship between membrane and flexure effects.

Based on this approach, a curved triangular element for the linear analysis of shells (thin or thick, shallow or deep) is presented in [11]. efficiency of this element to solve linear behaviour of curved structures (Fig.1 and Fig.2) was proven.

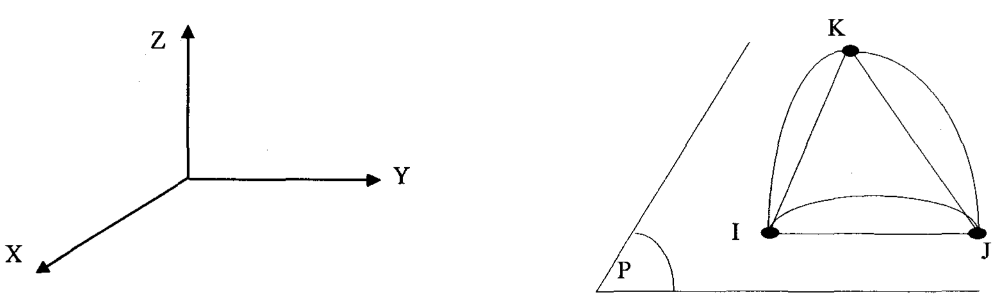

Fig.1. General idea of Marguerre's theory

THE DSTM TRIANGULAR CURVED SHELL ELEMENT

Introduction

Th shell element is a simple three nodes shallow element, with six degrees of freedom at each node. It has only corner nodes and is implemented in a cartesian coordinate system (Marguerre theory). It can be shown that such an element converges towards the deep shell solution [9]. The membrane strains are constant over the element. For the flexural behaviour, a discrete Mindlin-Reissner hypothesis is adopted. Due to the initial curvature, there is a coupling between the membrane and flexural behaviour at the element level. Special attention is paid to membrane and shear locking phenomenon.

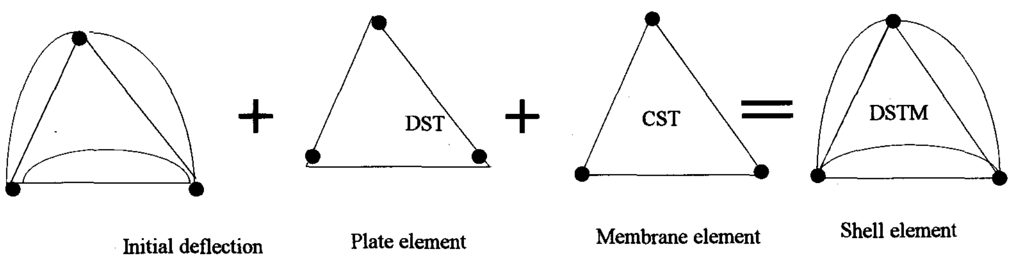

Fig.2. Construction stapes of the DSTM element

Reference Configuration Area - Coordinates

The element is built into a set of axes bound to the element. The x and y axes are in the plane of the triangle (Fig.3).

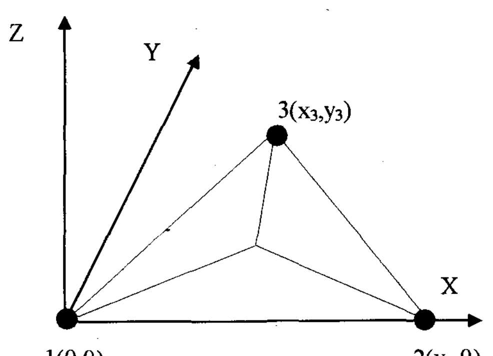

Fig.3. Area coordinates and axes of the element

The x axis is parallel to the first side. The z axis is perpendicular to the plane of the triangle. The area coordinates are defined by the following relations (Fig.3) :

$$L_1 = \text{Area}\frac{p_{23}}{A} \quad ; \quad L_2 = \text{Area}\frac{p_{13}}{A} \quad ; \quad L_3 = \text{Area}\frac{p_{12}}{A} \tag{3}$$

Where A is the area of the triangle. The area coordinates L_1 , L_2 , L_3 are dependent :

$$L_1 + L_2 + L_3 = 1 \tag{4}$$

They can be expressed as a function of the cartesian coordinates as follows:

$$L_1 = \frac{\left(x_2.y_3 - x.y_3 + y.\left(x_3 - x_2\right)\right)}{2.A} \; , L_2 = \frac{\left(x.y_3 - y.x_3\right)}{2.A} \; , \; L_3 = \frac{\left(y.x_2\right)}{2.A} \tag{5}$$

L_2 and L_3 will be chosen as independent variables here in the following relation holds :

$$\begin{Bmatrix} \frac{\partial}{\partial x} \\ \frac{\partial}{\partial y} \end{Bmatrix} = \frac{1}{2.A}\begin{bmatrix} y_3 & 0 \\ -x_3 & x_2 \end{bmatrix}\begin{Bmatrix} \frac{\partial}{\partial L_2} \\ \frac{\partial}{\partial L_3} \end{Bmatrix} \tag{6}$$

The Membrane Behaviour

The membrane is the classical Turner's element [12]. The displacements are linear and the strains are constant over the triangle :

$$\begin{Bmatrix} u \\ v \end{Bmatrix} = \begin{bmatrix} L_i & 0 \\ 0 & L_i \end{bmatrix}\begin{Bmatrix} u_i \\ v_i \end{Bmatrix} \tag{7}$$

$$\begin{Bmatrix} \varepsilon_x \\ \varepsilon_y \\ \gamma \end{Bmatrix} = \begin{bmatrix} L_{i,x} & 0 \\ 0 & L_{i,y} \\ L_{i,y} & L_{i,x} \end{bmatrix}\begin{Bmatrix} u_i \\ v_i \end{Bmatrix} \tag{8}$$

There are six displacement and three strain parameters.

Another way of building the element is to calculate the strain ε_i of the three sides and then to express the strains ε_x , ε_y , γ as a function of ε_i (Fig.4):

$$\begin{Bmatrix} \varepsilon_1 \\ \varepsilon_2 \\ \varepsilon_3 \end{Bmatrix} = \begin{bmatrix} m_1^2 & n_1^2 & m_1 n_1 \\ m_2^2 & n_2^2 & m_2 n_2 \\ m_3^2 & n_3^2 & m_3 n_3 \end{bmatrix} \begin{Bmatrix} \varepsilon_x \\ \varepsilon_y \\ \gamma \end{Bmatrix} \tag{9}$$

where m_i and n_i are the direction cosines of the edge i. This relationship can be inverted.

The two methods give identical results. This is obvious since the strains are constant over the triangle.

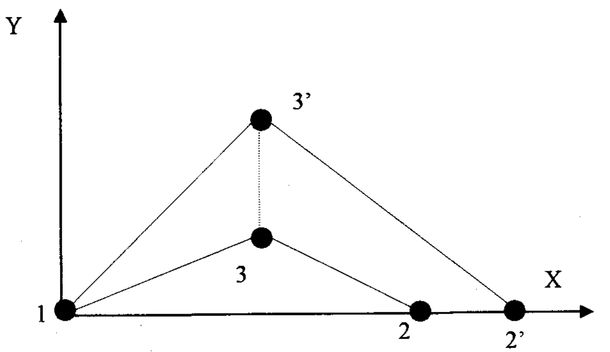

Fig.4. Strain {ε} of the three sides

The Flexural Behaviour

The flexural element formulation, which is fully described in [7] and [13], is based upon a Discrete Strain Theory (DST). The principles of this element will be briefly discussed here.

Some aspects of the theory of isotropic plates with transverse shear

a) Kinematics

In the Mindlin/Reissner or shear plate theory the assumption that "normals of the mid-surface of the undeformed plate remain straight but not necessarily normal to the mid-surface of the deformed plate" leads to the following definition of the displacement components u, v, w in the x, y and z Cartesian coordinate system.

$$u = z\beta_x(x,y) \qquad v = z\beta_y(x,y) \qquad w = w(x,y) \tag{10}$$

where x and y are coordinates of the reference middle surface, z is the coordinate through the thickness h :

$$-\frac{h}{2} \le z \le \frac{h}{2} \tag{11}$$

w is the transverse displacement. β_x and β_y represent the rotations of the normal to the x-z and y-z planes, respectively. If we introduce the rotations θ_x and θ_y around the x and y axes then :

$$\theta_x = -\beta_x \qquad\qquad \theta_y = \beta_x \tag{12}$$

The bending strains ε_b and curvatures $\langle\chi\rangle$ are given by

$$\langle\varepsilon_b\rangle = z\langle\chi\rangle \tag{13}$$

with :

$$\langle\chi\rangle = \langle\beta_{x,x} \quad \beta_{y,y} \quad \beta_{x,y} + \beta_{y,x}\rangle \tag{14}$$

whereas the transverse shear strains are given by:

$$\langle\gamma\rangle = \langle\gamma_{xz} \quad \gamma_{yz}\rangle = \langle w_{,x} + \beta_x \quad w_{,y} + \beta_y\rangle \tag{15}$$

b) Constitutive equations

For an isotropic material the in-plane stresses are related to the bending strains by

$$\{\sigma\} = [D]\{\varepsilon_b\} = z[D]\{\chi\} \tag{16}$$

with

$$\{\sigma\} = \langle\sigma_x \quad \sigma_y \quad \sigma_{xy}\rangle \tag{17}$$

$$[D] = \frac{E}{(1-\nu^2)}\begin{bmatrix} 1 & \nu & 0 \\ \nu & 1 & 0 \\ 0 & 0 & \frac{1-\nu}{2} \end{bmatrix} \tag{18}$$

E and ν are Young's modulus and Poisson's ratio.

The bending moments {M} and shear forces {T} are related to the strain resultants $\{\chi\}$ *and* $\{\gamma\}$ by Fig.5.

$$\{M\}=[D_b]\{\chi\} \qquad \{T\}=[D_s]\{\gamma\} \tag{19}$$

$$\text{with : } \quad \langle M\rangle=\langle M_x \quad M_y \quad M_{xy}\rangle \qquad \langle T\rangle=\langle T_X \quad T_y\rangle \tag{20}$$

$$[D_b]=\frac{h^3}{12}[D] \qquad [D_s]=kGh[I] \tag{21}$$

k is the shear correction factor (a value of 5/6 is usually considered for homogeneous isotropic plates) and the shear modulus is :

$$G=\frac{E}{2(1+\nu)} \tag{22}$$

c) Equilibrium equations

The equilibrium equations on the middle surface A are given by:

$$T_{x,x}+T_{y,y}+p(x,y)=0 \quad , \quad M_{x,x}+M_{xy,y}-T_x=0 \quad , \quad M_{y,y}+M_{yx,x}-T_y=0 \tag{23}$$

where p(x,y) is the distributed load per unit mid-surface acting in the Z direction.

d) Shear influence factor f

Equations (10)-(23) for an isotropic plate lead to the following relations :

$$\gamma_{xz}=\frac{T_x}{D_s}=\frac{1}{D_s}\left(M_{x,x}+M_{xy,y}\right) \quad , \quad \gamma_{yz}=\frac{T_y}{D_s}=\frac{1}{D_s}\left(M_{xy,x}+M_{y,y}\right) \tag{24}$$

$$\text{or : } \quad w_{,x}+\beta_x=fx\left(\beta_x,\beta_y\right) \quad , \quad w_{,y}+\beta_y=fy\left(\beta_x,\beta_y\right) \tag{25}$$

$$\text{with : } \quad \begin{aligned} fx&=\frac{D_b}{D_s}\left(\beta_{x,xx}+\nu\beta_{y,xy}+\frac{1-\nu}{2}\left(\beta_{x,yy}+\beta_{y,xy}\right)\right)\\ fy&=\frac{D_b}{D_s}\left(\beta_{y,yy}+\nu\beta_{x,xy}+\frac{1-\nu}{2}\left(\beta_{x,xy}+\beta_{y,xx}\right)\right)\end{aligned} \tag{26}$$

and : $$D_b = \frac{Eh^3}{12(1-\nu^2)} \qquad D_s = k.G.h \tag{27}$$

f_x and f_y which, represent the influence of the transverse shear through the shear influence factor ϕ,are given by the following equations:

$$fx = \phi.FX(\beta_x,\beta_y) \qquad fy = \phi.FY(\beta_x,\beta_y) \tag{28}$$

with : $$\phi = \frac{D_b}{L^2 D_s} = \frac{E}{kG}\left(\frac{h}{L}\right)^2 \tag{29}$$

where L is the characteristic length of plate.

e) Stain energy

The strain energy for an element with an of area A is given by

$$U^e = U_b^e + U_s^e \tag{30}$$

$$U_b^e = \frac{1}{2}\int_{A^e} \langle X\rangle [D_b]\{X\} dA \quad , \quad U_s^e = \frac{1}{2}\int_{A^e} \langle \gamma\rangle [D_s]\{\gamma\} dA \tag{31}$$

where $<\chi>$, $<\gamma>$, $[D_b]$, $[D_s]$ are given by equations (14), (15) and (21), respectively.

The Euler-Lagrange equations associated with the use of the total potential energy are the three equilibrium equations (23) expressed in terms of w, β_x and β_y. A C° continuity for w, β_x and β_y is required for a fully compatible element.

For an isotropic material, Equation (31) can be expressed in terms of ϕ (29) as follows.

$$U_s^e = \frac{1}{2\phi}\frac{D_b}{L^2}\int_A \left(\left(w_{,x} + \beta_x\right)^2 + \left(w_{,y} + \beta_y\right)^2 \right) dA \tag{32}$$

This expression depends on the factor ϕ^{-1}. The shear locking can occur if the displacement w and the independent rotations fields β_x and β_y do not satisfy the following equations:

$$\gamma_{xz} = w,_x + \beta_x \rightarrow 0 \quad , \quad \gamma_{yz} = w,_y + \beta_y \rightarrow 0 \qquad \text{for } \phi \ll 1 \qquad (33)$$

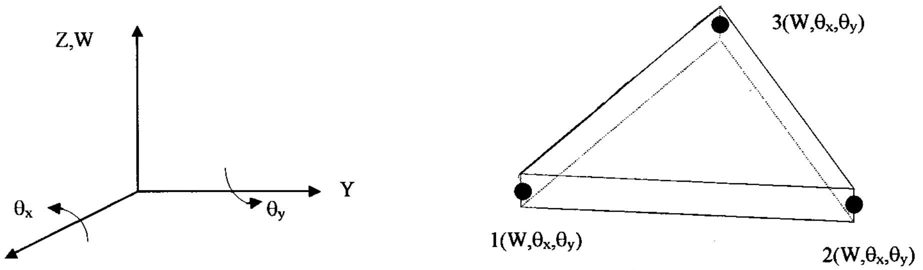

Nine D.O.F Triangular plate bending element

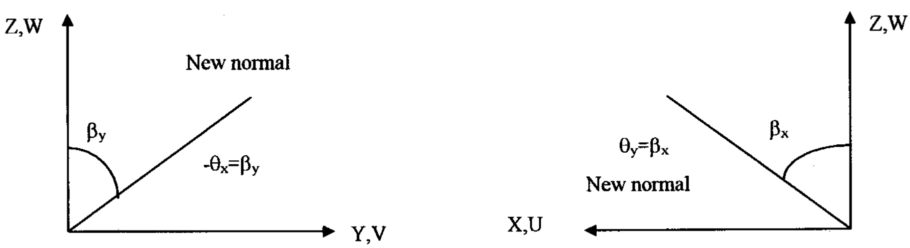

Y-Z Plane **Z-X Plane**

Positive directions of β_x and β_y

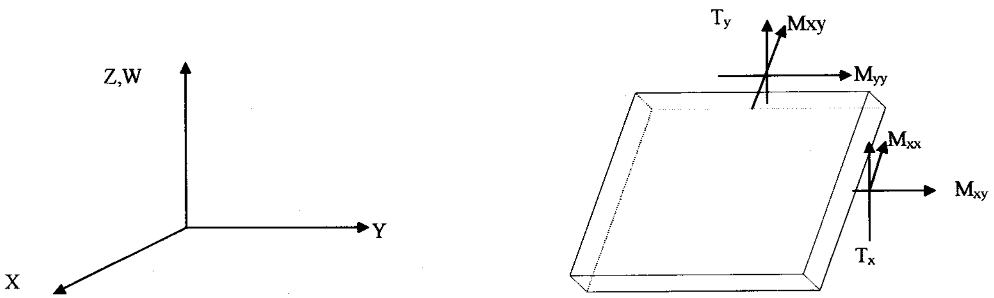

Bending Moments and Shear forces

Fig.5 Flexural behaviour of plate

If the equilibrium equations (23) are satisfied explicitly on the continuum, w, β_X and β_Y are related through equations (25). In this case the shear strain energy is given by:

$$U_s^e = \frac{1}{2}\int_A D_s\left(\left(w_{,x}+\beta_x\right)^2+\left(w_{,y}+\beta_y\right)^2\right)dA \qquad (34)$$

with equations (25) to (29)

$$w_{,x}+\beta_x = \phi.FX\left(\beta_x,\beta_y\right) \quad , \quad w_{,y}+\beta_y = \phi.FY\left(\beta_x,\beta_y\right) \qquad (35)$$

$$\text{or : } \quad U_s^e = \frac{1}{2}\int_A D_s\left(fx^2+fy^2\right).dA = \frac{1}{2}\phi\frac{D_b}{L^2}\int_A\left(FX^2+FY^2\right).dA \qquad (36)$$

This shear energy expression depends on the factor ϕ and converges to zero if ϕ<<1 (no shear locking)

The formulation of the discrete shear triangle element dst

The following ideas are kept in mind when looking for a new element :

1. If the transverse shear effects are negligible compared to the bending effects, the element should coincide with DKT, i.e.

   DST ----------> DKT if ϕ << 1

therefore,

2. The element has 9 D.O.F only. The displacements w and rotations β_X and β_Y of the normal (and Mindlin boundary conditions can be applied) : are given by the following equation.

$$\langle U\rangle = \left\langle\left(w_i \quad \beta_{xi} \quad \beta_{yi}\right)_{i=1,2,3}\right\rangle \qquad (37)$$

with : $\quad \theta_{xi} = -\beta_{yi} \qquad \theta_{yi} = \beta_{xi}$

3. The formulation of the stiffness matrix of DST element is such that :

a) the strain energy is given by equations (30), (31) and (36).

$$U^e = U_b^e + U_s^e \tag{38}$$

$$U_b^e = \frac{1}{2}\int_{A^e} \langle \chi \rangle [D_b] \{\chi\} dA \quad , \quad U_s^e = \frac{1}{2}\int_{A^e} \langle F \rangle [D_s] \{F\} dA \tag{39}$$

$$\langle \chi \rangle = \langle \beta_{x,x} \quad \beta_{y,y} \quad \beta_{x,y} + \beta_{y,x} \rangle \tag{40}$$

$$\langle F \rangle = \langle FX \quad FY \rangle \tag{41}$$

$FX(\beta_X , \beta_y)$ and $FY(\beta_X , \beta_y)$ are given by equation (26)

b) β_X (x,y) and β_y (x,y) are described by C° quadratic interpolation functions Fig.6:

$$\beta_x = \sum_{i=1}^{6} N_i(\xi,\eta)\, \beta_{x_i} \quad , \quad \beta_y = \sum_{i=1}^{6} N_i(\xi,\eta)\, \beta_{y_i} \tag{42}$$

β_X and β_y are the nodal values at the corner 1, 2, 3 and mid-nodes 4, 5, 6 (Fig.6), $N_i(\xi,\eta)$ are :

$$\begin{aligned} N_1 &= \lambda(2\lambda - 1) \quad , \quad N_2 = \xi(2\xi - 1) \quad , \quad N_3 = \eta(2\eta - 1) \\ N_4 &= 4\xi\eta \quad\quad\quad , \quad N_5 = 4\eta\lambda \quad\quad , \quad N_6 = 4\xi\lambda \end{aligned} \tag{43}$$

with $\lambda = 1 - \xi - \eta$

c) a linear variation of β_n is imposed along the sides (Fig.7):

$$\left(\beta_n\right)_k = \frac{\left[\left(\beta_n\right)_i + \left(\beta_n\right)_j\right]}{2} \qquad k = 4,5,6 \tag{44}$$

d) equation (35) represents the bending equilibrium equations and the constitutive relations are represented as follows:

(i) at the corner nodes 1, 2, 3 :

$$w_{,x} + \beta_x = fx\left(\beta_x , \beta_y\right) \quad , \quad w_{,y} + \beta_y = fy\left(\beta_x , \beta_y\right) \tag{45}$$

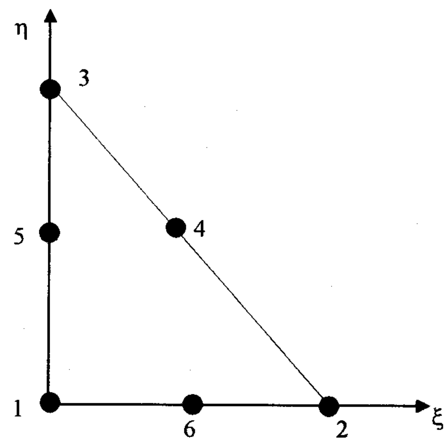

Fig.6 Refence element

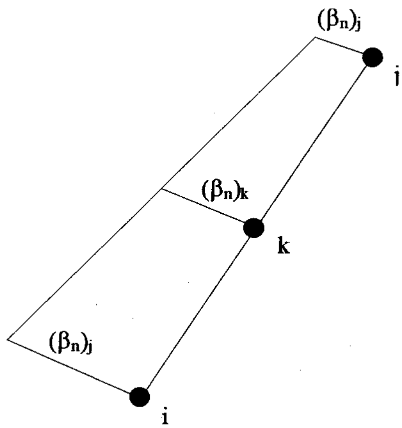

Fig.7 Interpolation of the normal rotation β_n linear

(ii) at the mid-side points 4, 5, 6

$$\left(w_{,s}\right)_k + \left(\beta_s\right)_k = -S_k . fx + C_k . fy \qquad k = 4,5,6 \tag{46}$$

Assuming a cubic Hermite variation of W(s) along each side (Fig.8) :

$$\left(w_{,s}\right)_k = -\frac{3\left(w_i - w_j\right)}{2l_{ij}} - \frac{\left(w_{,s}\right)_i}{4} - \frac{\left(w_{,s}\right)_j}{4} \tag{47}$$

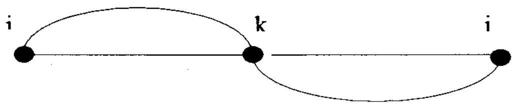

Fig.8 Interpolation of the transversal displacement Cubic Hermit variation of W_s

along each side ij we have (Fig.9 and Fig.10):

$$w_{,s} = C_k . w_{,y} - S_k . w_{,x} \quad , \quad \begin{Bmatrix} \beta_n \\ \beta_s \end{Bmatrix} = \begin{bmatrix} C_k & S_k \\ -S_k & C_k \end{bmatrix} \begin{Bmatrix} \beta_x \\ \beta_y \end{Bmatrix} \tag{48}$$

$$\text{with :} \quad S_k = sin\gamma_{ij} \quad ; \quad C_k = cos\gamma_{ij} \quad ; \quad \gamma_{ij} = \left(x, n_{ij}\right) \tag{49}$$

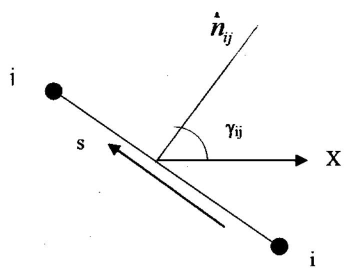

Fig.9 The angle γ between the normal to the ij side and X- axis

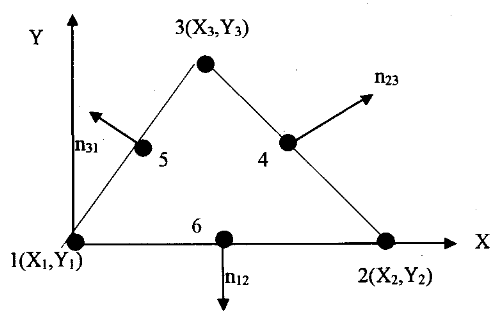

Fig.10 The three normals to the three sides

twenty-one variables have been introduced (12 β's and 9 W's) for a total of 12 relations (equations (44)-(46)). Twelve variables are eliminated : the rotations of the middle surface $W_{,x}$ and $W_{,y}$ at the corner nodes and the rotations of the normal β_n and β_s at the mid-nodes. They are expressed in terms of the final 9 D.O.F W, β_x and β_y at the corner nodes (equation (37)).

β_{sk}, FX, FY, β_x and β_y ,can be expressed in terms of {U}using the following equation[11]

$$\beta_{sk} = \langle H_s(k)\rangle\{U\} \qquad k = 4,5,6$$
$$FX = \langle HFX\rangle\{U\} \qquad ; FY = \langle HFY\rangle\{U\} \tag{50}$$

$$\beta_x = \langle H_x(\xi,\eta)\rangle\{U\} \quad , \quad \beta_y = \langle H_y(\xi,\eta)\rangle\{U\}$$

The curvatures $\{\chi\}$ (equation (14)) are given by : $\{\chi\} = [B_b]\{U\}$ (51)

$$\text{with } :[B_b(\xi,\eta)] = \frac{1}{2A}\begin{bmatrix} y_{31}\langle H_{x,\xi}\rangle + y_{12}\langle H_{x,\eta}\rangle \\ -x_{31}\langle H_{y,\xi}\rangle - x_{12}\langle H_{y,\eta}\rangle \\ -x_{31}\langle H_{x,\xi}\rangle - x_{12}\langle H_{x,\eta}\rangle + y_{31}\langle H_{y,\xi}\rangle + y_{12}\langle H_{y,\eta}\rangle \end{bmatrix} \tag{52}$$

where $2A = x_{31}.y_{12} - x_{12}.y_{31}$, $\rangle H_{x,\xi}\langle$, $\rangle H_{x,\eta}\langle$, $\rangle H_{y,\xi}\langle$, $\rangle H_{y,\eta}\langle$ are the erivatives of $< H_x >$ and $<H_y>$ (equations (50)) with respect to the area coordinates.

The shear strains < F > (equation (39)) are given by

$$\{F\} = \begin{Bmatrix} FX \\ FY \end{Bmatrix} = [B_s]\{U\} \tag{53}$$

$$\text{with} \qquad : [B_s] = \begin{bmatrix} \rangle HFX\langle \\ \rangle HFY\langle \end{bmatrix} \tag{54}$$

The stiffness matrix [K] is the sum of the bending and the shear stiffness matrices.

$$[K] = [K_b] + [K_s]$$
$$[K_b] = 2A\int_0^1\int_0^{1-\eta}[B_b]^T[D_b][B_b]d\xi,d\eta \tag{55}$$
$$[K_s] = A[B_s]^T[D_s][B_s]$$

with $[B_b]$, $[B_s]$ given by equations (52), (54) and $[D_b]$ and $[D_s]$ by equations (21).

An exact integration of $[K_b]$ is obtained using three Hammer numerical integration points.

Once the nodal variables {U} (equation (37) are known, the bending moment {M} can be evaluated at any point by (19), (51):

$$\{M(\xi,\eta)\} = [D_b][B_b(\xi,\eta)]\{U\} \tag{56}$$

The constant shear forces T_x and T_y are given by (19), (53)

$$\{T\} = [D_s][B_s]\{U\} \tag{57}$$

The in-plane stresses σ_x , σ_y and σ_{xy} are obtained at any point by (16), (51):

$$\{\sigma(\xi,\eta,z)\} = z[D_b][B_b(\xi,\eta)]\{U\} \tag{58}$$

A realistic distribution of transverse shear stresses σ_{xz} and σ_{yz} is usually obtained in Mindlin and Kirchhoff plates by considering the homegeneous stress equilibrium equations:

$$\sigma_{xz,z} = \sigma_{x,x} - \sigma_{xy,y} \quad , \quad \sigma_{yz,z} = \sigma_{y,y} - \sigma_{xy,x} \tag{59}$$

Coupling Between Membrane and Flexural Behaviour

The present element (DSTM) is not flat. The initial curvature is taken into account by Marguerre's theory. It is a shallow shell theory developed in cartesian coordinates. It can be shown that such an element converges towards the deep shell solution [9]. This is not the case for an element developed in curvilinear coordinates with a shallow shell theory [9].

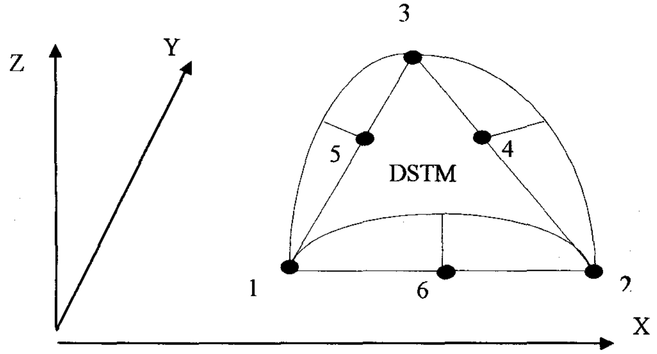

Fig.11 The DSTM element

NUMERICAL EXAMPLES

A number of commonly used benchmark problem are examined to compare the performance the present element with that of other element models in the literature. Elements to be included in the comparisons are summarized as follows.

Name	Element Description
ANS4	Four nodes shell element based on assumed covariant strains [14]
ANS9	Nine nodes shell element based on assumed covariant strains [14]
ANST3	Three nodes shell element based on assumed covariant strains [15]
ANST6	Six nodes shell element based on assumed covariant strains [15]
ECB1	A three nodes deep shell theory [15]
ECB2	ECB2 : A three nodes shallow shell theory [15]
DKTM	DKTM : A three nodes shallow shell element based on marguerre's theory [1]

Cantilever Beam Under Concentrated Load

A contilever beam of a rectangular cross-section, is subjected to a concentreted load at its free end as shown in Fig.E1. This problem is proposed to assess the effect of the transverse shear introduced discreteley on the structure behaviour. The analytic solution in the direction of the out-of-plane load is :

$$w = \frac{12\,P\,L^3}{3\,E\,b\,h^3}\left[1+\frac{1}{2\,k}\left(\frac{h}{L}\right)^2\right] \quad if \quad \frac{h}{L}\langle\langle 1 \;\Rightarrow\; w \approx \frac{4\,P}{E\,b}\left(\frac{L}{h}\right)^3$$

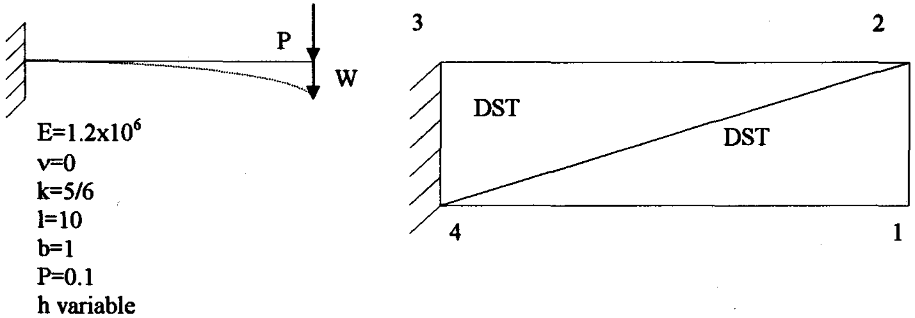

Fig.12. Cantilever beam under concentrated load

In a first analysis we have examined three cases of this cantilever beam in function of the ratio h/l (h/l=0.01, 0.2, 1). Using the mesh size presented in the Fig.12. Results of the DSTM element are compared with those DKTM element and those of the analytical solution.

a- The thin plate case h/l=0.01

The numerical results for this case indicate that the element is free from the shear locking phenomena.

Theoretical solution	DKTM	DSTM
0.333	0.31327	0.31329

b- The moderate plate case

In the same maner as in the case (a), the cantilever beam is modelled by two elements with (DSTM, DKTM, ANST3) elements. The results of the DSTM and ANST3 elements are better than the DKTM element, because these elements incorporate the effect of the transverse shear.

Theoretical solution	DKTM	DSTM	ANST3
4.3×10^5	3.915×10^5	4.012×10^5	4×10^5

c- The thick plate case

In this case the result of the DKTM element is very poor. while the DSTM result is very good.

Theoretical solution	DKTM	DSTM
5.33×10^5	3.13×10^5	5.128×10^5

d- In a second analysis, the same cantilever beam is analysed with the DKTM, DSTM and ANST6 elements as a function of the h/l ratio. Results of the different elements are presented in the following table. They indicate that the proposed element performs well in both thin and thick plate cases.

l/h

W	5	4	3	2	1
DKTM	0.39	0.20	0.84	0.25	0.31
DSTM	0.40	0.20	0.90	0.29	0.51
ANST6	0.42	0.22	0.96	0.30	0.53
Theoretical solution	0.426	0.221	0.96	0.306	0.533

Pinched Cylinder Problem

The pinched cylinder is a classical problem that has been used extensively to check the ability of shell elements to represent the inextensionel bending deformation. The open-end cylinder leads to the pure inextentional deformation at the limit as t/R approaches zero. An analytic solution for this limiting case is given by [16] which is 0.1139. Fig.13 shows the model geometry. Using symmetry, only one eigth of the cylinder was actually analyzed. Normalized transverse displacements under the load are given on Fig.14 for different mesh sizes. Numerical results for the pinched cylinder with open ends indicate that the proposed element exhibits a good accuracy.

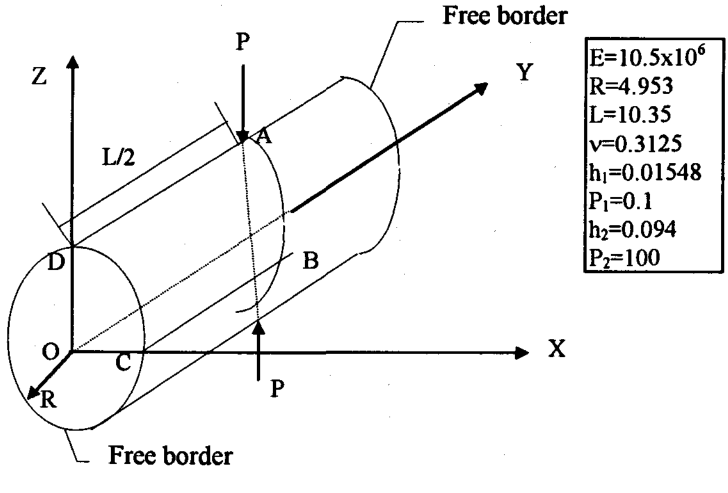

Fig.13. Pinched cylinder with free edges

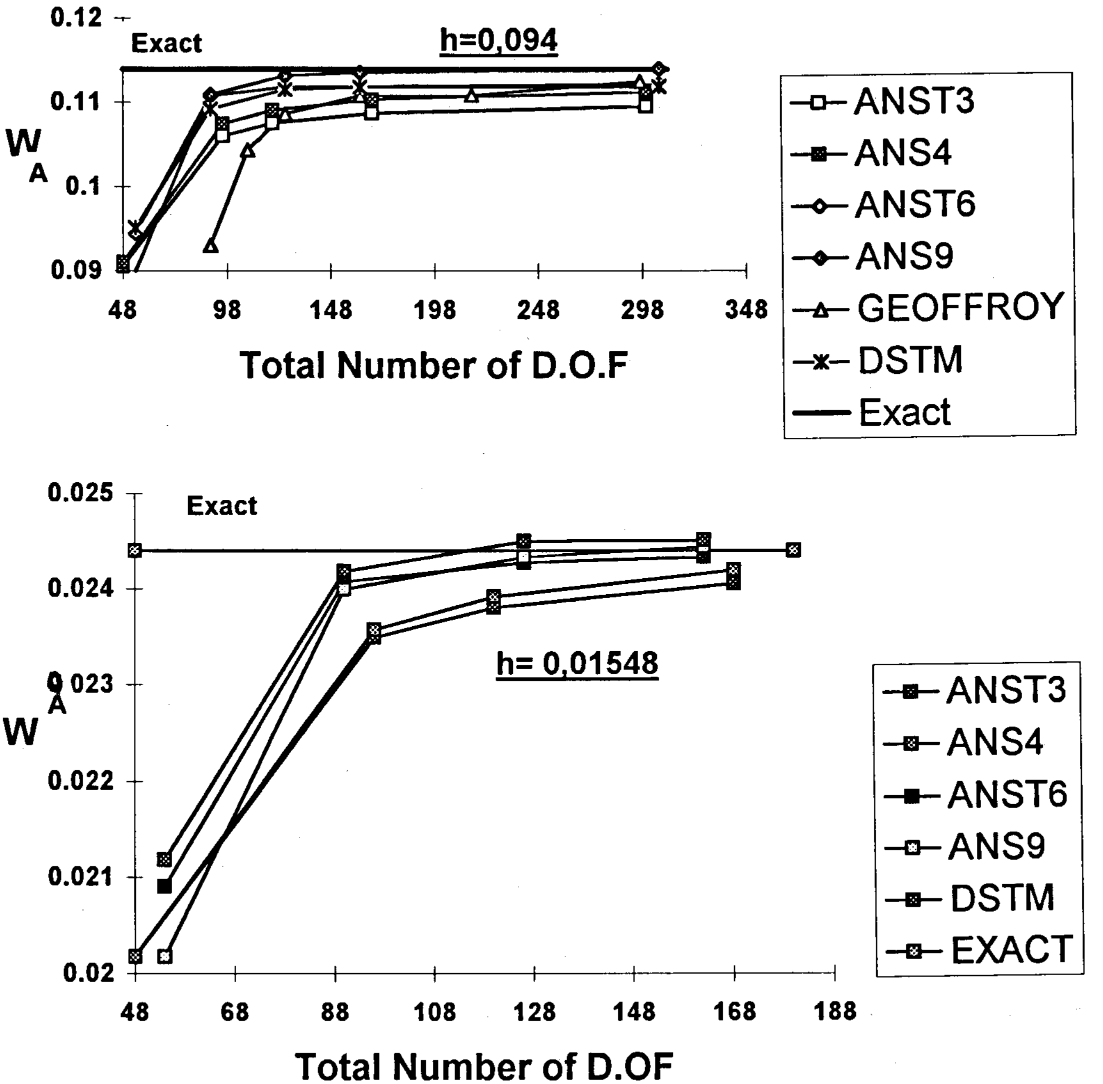

Fig.14. Pinched cylinder problem transverse displacement under the load

TRANSVERSE DISPLACEMENT AT NODE A

Meshes	ANST6	ANS9	DSTM
3x3	0.8288	0.7896	0.8350
6x3	0.9727	0.9738	0.9587
7x3	0.9815	0.9937	0.9794
9x3	0.9825	0.9967	0.9820
17x3	0.9853	1.000	0.9822

RADIAL DISPLACEMENT AT NODE B

Meshes	ANST6	ANS9	DSTM
3x3	0.9367	0.8958	0.8720
6x3	0.9987	0.9943	0.9800
7x3	1.000	1.001	0.9940
9x3	1.000	0.9994	0.9960
17x3	0.9998	1.001	0.9970

Infinitely Long Pinched Cylinder

The infinitely long pinched circular cylinder, presented in Fig.15, is subjected to two uniform transverse load lines. We seek to solve this problem to demonstrate the influence of the relationships between deformations and displacements on one hand and to follow DSTM element behaviour while modeling thick curved structures ($R/h = 10$) on the other hand. The geometrical and mechanical data of this shell are presented in figure Fig.15. In the same manner as in [15], we model on the basis of symmetry a quarter of a shell strip considering several cuttings (Fig.15). Conditions of the imposed limits allow us to get rid of the Y direction influence over the deformation of the whole. The uniform load is replaced with concentrated forces.

The numerical results of normal displacements for A and B nodes, according to the total number of degrees of freedom (D.O.F.), are presented on Fig.16. The

DSTM results are compared with two exact solutions. One of them is given by Donnel (solution based on the shallow shell theory)while the second one, is given by Koiter and Sander (solution based on the deep shell theory). The numerical results are shown in [15] (The ECA elements, the ECB2 element based on the shallow shell theory and the ECB1 element based on the deep shell theory) along with elements developped in [15].

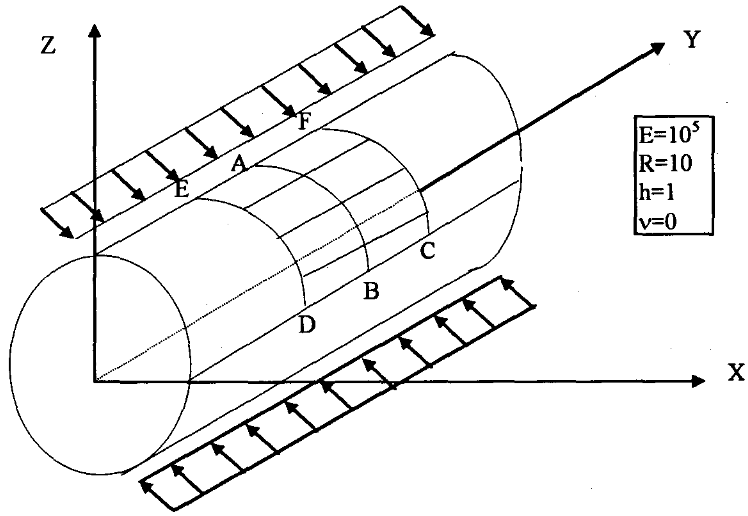

Fig.15. Infinitely long pinched cylinder

It is worth noting that:
- A rapid monotonous convergence towards the exact solution is obtained for DSTM element by the theory of deep shells.
- DSTM element and ANS elements [15] are composed in the same way.
- We notice the existence of a jump between the two first mesh sizes and the third one.

This is due to the fact that the shell behaves as shallow one for the two first meshes while it shows a deep shell behaviour if the mesh is refined.

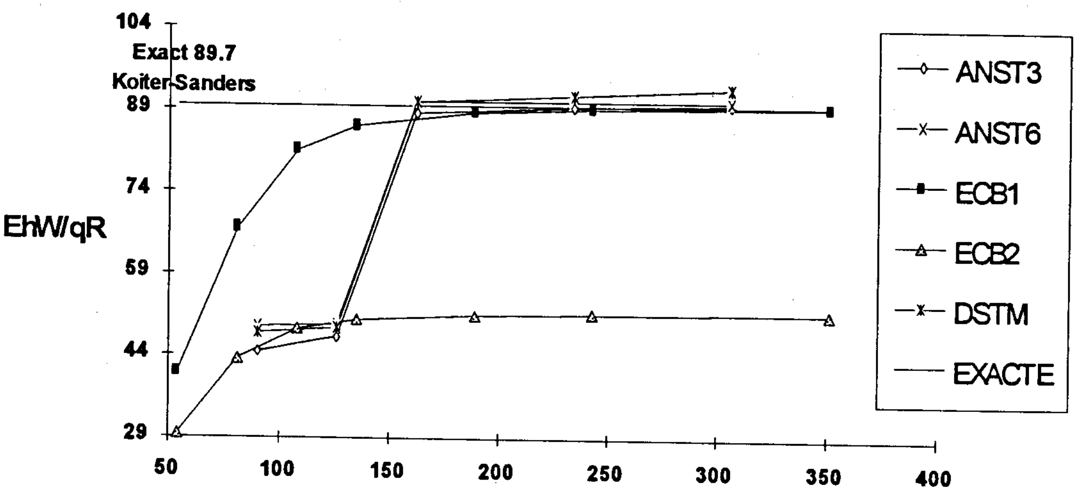

Fig. 16. Infiniteley long pinched cylinder
Normal Displacement at A

Hemispherical Shell Problem

A hemispherical shell, which is subjected to self-equilibrating radial point forces at 90° intervals, is analyzed via the quarter model shown in Fig.17. This problem is intended to check the element performance for the rigid body rotations and the near extensional bending of a doubly curved shell. The geometry and material properties are shown in Fig.17. An analytical solution for the problem is given by Flugge [17]. The reference solution for the radial displacement at the loaded points is 0.0924. One quarter of the hemisphere was actually analyzed using the symmetry of the structure. Results for the different mesh sizes are presented in the following table.They indicates that the proposed element performs well, while 4-ANS and ANST3 elements are locked due to the rigid body straining [15], [18]

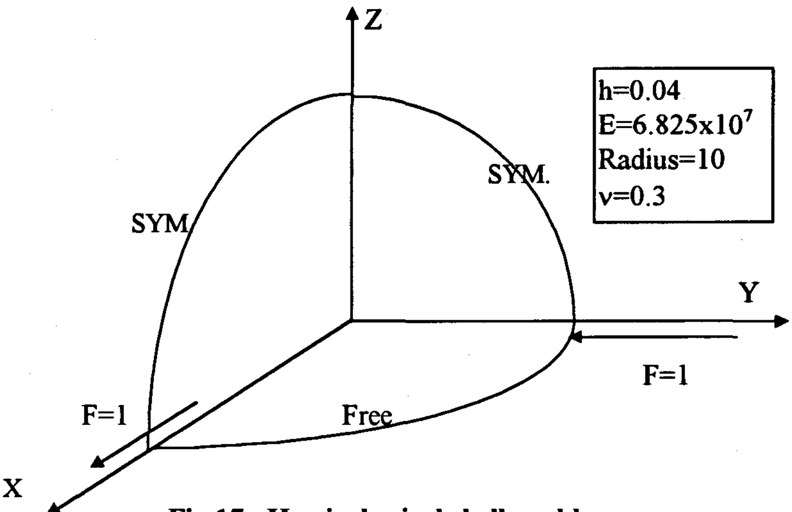

Fig.17. Hemispherical shell problem

Radial displacement at the loaded points

NODES/SIDES	ANST3	ANS4	ANST6	ANS9	DSTM
5 x 5	0.01321	0.02834	0.1310	0.6500	0.9900
9 x 9	0.04870	0.05698	0.7500	0.9653	0.9983

Patch-Test

Kirchhoff patch-test

The popular ' kirchhoff plate ' patch test is undertaken (Fig.18). A rectangular plate is subjected to the state of bending such that all three moment resultants are constant throughout the plate domain. The plate discretization consisting of four geometrically distinct DSTM elements yielded exact values for all three constant moments in each of the elements.

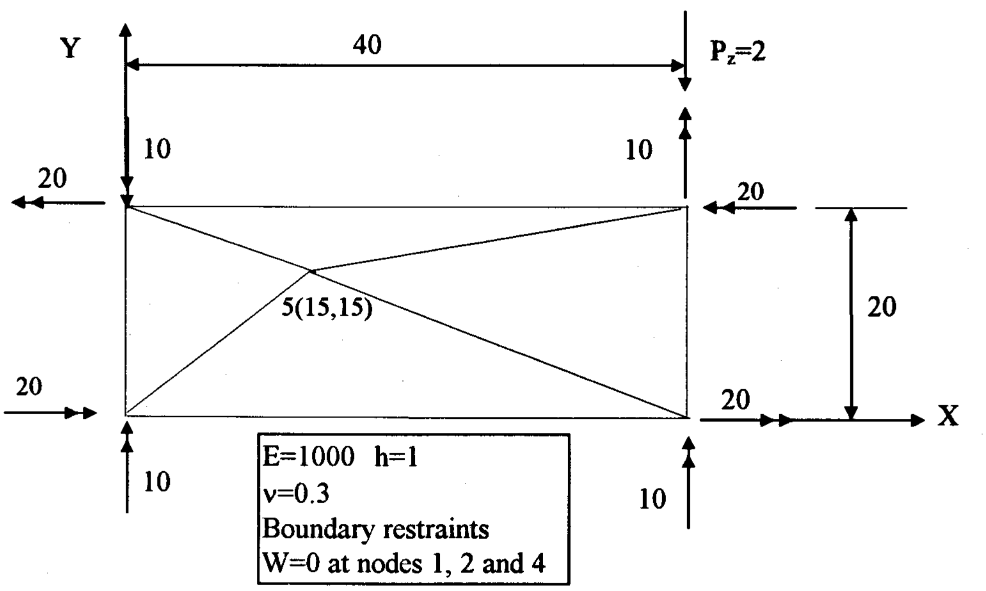

Fig.18. Kirchhoff patch-test

Shear patch-test

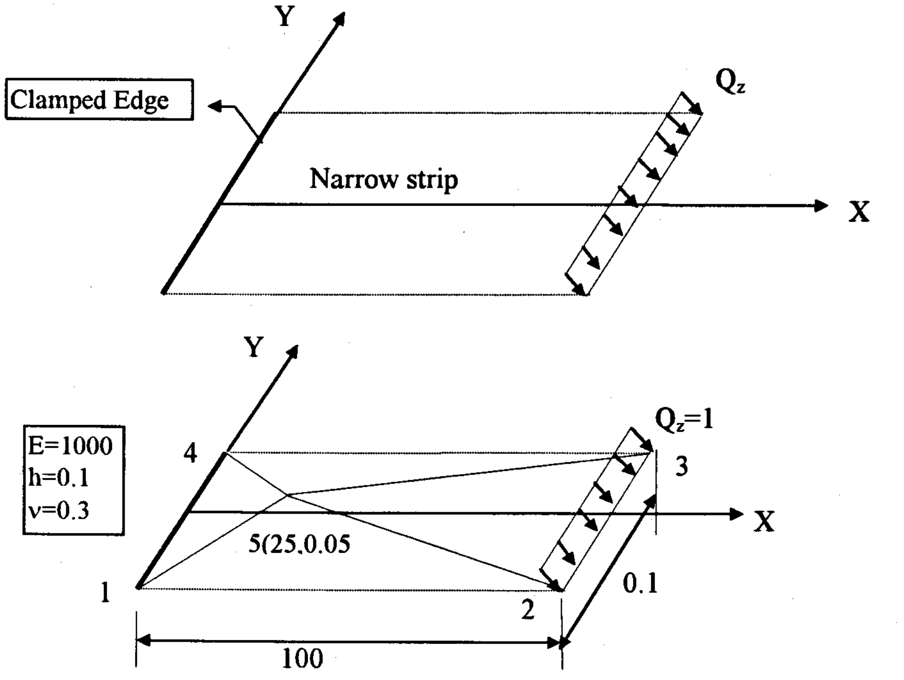

Fig.19. Transverse shear patch-test infinitely long cantilevered plate

Patch-test, inextensional bending modes

In order to test membrane locking, we performed the following test (Fig.E5) : A rectangular plate, with initial out-of-flatness, is subjected to constant bending, in the first case, the initial out-of-flatness is given by : $w_0 = \frac{4Hx}{L}\left(1 - \frac{x}{L}\right)$

and in the second case : $w_0 = \frac{Hxy}{BL}$

We analyse the test with H = 0.1 and 1. The analytical solution, according to Marguerre's theory, is given in [11]. In all the cases, the error is less than 1% for the energy. The maximum membrane stress is equal to 3 % of the flexural stress for H = 1, and is less than 1 % of the flexural stress for H=0.1.
It can be seen that the element does not lock. Without special attention being paid to membrane locking, results would have been be very poor.

Spectral And Eigenvalue Analysis Of Stiffness Matrix

Upon performing a spectral analysis of DSTM's stiffness matrix, six zero eigenvalues associated with the requisite rigid body modes are revealed. No spurious zero energy modes are present, as one would expect from an exactly integrated siffness matrix. Hence, the stiffness matrix is of a correct rank, and the element should be regarded as kinematically reliable.

CONCLUSION

The improvements realized in the present study include sufficient rank without transverse shear locking as well as consistent membrane strain interpolation. It permits in extensional bending and adequate representation of curvature effects allowing the capture of the important membrane-bending coupling. The obtained results confirm the efficiency of this approach (good convergence towards the analytical solution) for both deep and shallow shells as well as for thin or thick shell.

REFERENCES

1. **El Khaldi F ,1987,** Contribution au traitement des phénomènes de blocage de membrane et cisaillement dans la modélisation des arcs et des coques minces

en théorie de Marguerre Thèse de Doctorat, INSA de LYON, France, Janvier 87

2. **Belytschko T., Stolarski H. and Liu W.K., 1985** Stress projection for membrane and shear locking in shell finite elements Comp. Meth. Appl. Mech. Eng., 22, 697-722.

3. **Belytschko T., Wong B.L. and Stolarski H. ,1989** Assumed strain stabilization procedure for 9-node Lagrange shell element Int. J. Num. Meth. Eng., 28, 385-414

4. **Lee S.W.** and **Pain T.H.H ,1978** Improvement of plate and shell finite elements by mixed formulations AIAA Journal, 16, 29-34, 1978

5. **Parisch H. ,1979** A critical survey of the 9-node degenerated shell element with special emphasis on thin shell applications and reduced integration Comp. eth. App. Mech. Eng., 20, 323-250

6. **Hughes T.J.R., Cohen M. and Haroun M. ,1978** Reduced and selective integration techniques in the BATOZ J.L et LARDEUR P " A discrete shear triangular nine D.O.F element for the analysis of thick to very thin plates"

7. Int. J. Num. Meth. in Eng., Vol 28, N° 3, P 533-560, March 1989

8. **Choi C.K.** and **Kim S.H. ,1989** Coupled use of reduced integration and nonconforming modes in quadratic Mindlin elements Int. J. Num. Meth. Eng., 28, 1909-1929

9. Idelshon S. " Analyses statique et dynamique des coques par la méthode des éléments finis " Ph.D. thesis, Liège; 1974

10. **Stolarski H., Belytchko T., Carpenter** N. and **Kenndy J.M** " A simple triangular curved shell element for collapse analysis " Engineering Computation, Vol. 1, n° 3, PP 210-218, 1984

11. **Guenfoud M** " Présentation de l'élément DSTM pour l'analyse linéaire des coques d'épaisseur quelconque "Annalles de I.T.B.T.P ,N° 512, Mars 1993, France

12. **Turner M.J., Clough R.W., Martin H.C**. and **Topp L.J. ,1990** " Stiffness and deflection analysis of complex structures " J. Aero. Sci., 23, PP

805-823, 1956 BATOZ J.L et DHATT G " Modélisation des structures par éléments finis, Poutres et Plaques " Hermès, Paris,

13. **Park K.C** and **Stanley G.M, 1986** A curved C° shell element based on assumed natural-coordinate strains J. of Applied Mechanics, ASME, 53, 278-290

14. **Guenfoud M, 1990** Deux éléments triangulaires nouveaux pour l'analyse lineaire et non lineaire géométrique des coques Thèse de Doctorat, INSA de LYON , FRANCE.

15. **Timoshenko S.** and **Woinwky-Krieger S. 1959** " Theory of plates and shells " 2nd Edition, McGraw-Hill, New York

16. **Flugge W., 1973** " Stresses in shells " 2nd Edition, Springer, Berlin

17. **Stanley G.M., 1985** Continuum-based shell analysis Ph.D. Dissertation, Stanford University, Stanfort, California